J Mater Sci (2008) 43:1811–1817
DOI 10.1007/s10853-007-2425-9

Prediction of ultrasonic wave velocities in sintered materials based on the ultrasonic properties of green or partially sintered compacts

K. K. Phani

Received: 2 August 2007 / Accepted: 17 December 2007 / Published online: 18 January 2008

Abstract This paper reports a new method of estimating ultrasonic properties of sintered materials from the ultrasonic properties of its powder compacts. The methodology is based on the observation that the ratio of ultrasonic shear wave velocity to longitudinal wave velocity is a function of porosity only and varies linearly with longitudinal velocity. The efficacy of the proposed method has been established with experimental data obtained from previously published studies. The method can be used as a potential tool for quality control of sintered products.

Introduction

In powder metallurgy and ceramic fields many engineering components are manufactured by sintering green powder compacts. This invariably leaves some amount of pores in the final product, which controls the physical behavior of components. Green compacts are prepared by various techniques like uniaxial pressing [1], uniaxial pressing followed by isostatic pressing [2], hot pressing [3] slip casting [4], etc. with the objective to control the amount, size, uniformity and distribution of porosity in the final product. During sintering densification takes place with a change in pore volume and morphology with consequent changes in ultrasonic and elastic properties. Monitoring of density change during the sintering process provides a tool for control of quality of the final product [5]. Thus ultrasonic velocity measurements have been widely used [4–10] as a non-destructive means to monitor the density or porosity changes in the material during sintering. This also allows moduli of materials to be evaluated at different stages of fabrication as a measure of product quality. It is well known [11] that ultrasonic velocity variation in porous material is dependent both on the amount of porosity and pore geometry. Thus porosity dependence of ultrasonic velocities and elastic properties of porous material have been the subject of extensive research over the last few decades leading to a large number of theoretical and empirical relations correlating porosity with ultrasonic velocities or moduli.

Theoretical relations are usually derived from the theories of two-phase composite materials by considering the stiffness of the included phase to be zero. The multiple scattering theories of Waterman and Truell [12] and Ying and Truell [13] have been widely used to treat the ultrasonic propagation characteristics of two-phase materials consisting of spherical scatterers. Sayers and Smith [14] have solved these equations numerically for porous solid but found that they give unphysical results for high porosity. They proposed a self-consistent theory which could be solved analytically and it gave reasonable behavior at high porosity. The self-consistent [15–18] and differential methods [19] have also been widely used in developing elastic moduli-porosity relations in porous solids. They essentially provide a method of approximately extending the exact analytical solution for small fraction of spherical or ellipsoidal pores to higher porosities. The application of these methods to real materials creates certain difficulties. Firstly, pores in real materials are highly irregular in shape, and their shape and morphology change with the progress in sintering. Secondly, microstructure must be precisely known before a particular relation can be used to estimate either velocity or elastic moduli. Thus these relations can

K. K. Phani (✉)
Central Glass & Ceramic Research Institute, Kolkata 700032, India
e-mail: kkphani@cgcri.res.in

only be useful in analyzing post-sintering behavior when the microstructural details are known from the sintered product. They fail to predict velocity or moduli values based on microstructural analysis of the green compacts alone.

Several empirical relations have also been proposed to analyze ultrasonic velocity or elastic moduli variation with porosity. A comprehensive account of these relations has been given by Rice [11] and the references mentioned therein. These relations serve the useful purpose of analyzing the post-sintering behavior, but they fail to provide any information regarding pore character to predict ultrasonic velocity or elastic moduli for a given value of porosity or pore morphology. From a metallurgist's or ceramist's point of view, it would be ideal if it can be assessed during the preparation of green compact itself whether a desired property can be achieved at a specified amount of porosity with the pore morphology that will evolve during the sintering process. This will have two fold advantages—firstly, the properties of green compact can be engineered by modifying the powder processing to produce material with specified properties. Secondly, it can be used as quality control tool to eliminate compacts which will not yield the desired product, thereby avoiding costly sintering process.

The aim of the present paper is to develop a semi-analytical procedure based on the theories of physical acoustics and to predict ultrasonic velocity variation with densification during sintering from the ultrasonic properties of green compacts. It may be mentioned here that sometimes the measurement of ultrasonic properties of green compacts creates difficulties due to fragility of the compact. In that case the method can be used by utilizing ultrasonic properties of partially sintered compacts. The applicability of the method has been evaluated in terms of experimental data reported in the literature.

Analytical procedure

The following assumptions are made in deriving the analytical procedure :

a. Pores are randomly distributed and oriented so that the material can be considered isotropic on a macroscopic scale.
b. Pores are filled with air whose bulk modulus is negligible.

The theory of physical acoustics gives the relation between ultrasonic longitudinal velocity, V_L, shear wave velocity, V_T, and Poisson's ratio as [20]

$$v = \frac{1 - 2\left(\frac{V_T}{V_L}\right)^2}{2\left(1 - \left(\frac{V_T}{V_L}\right)^2\right)} \quad \text{or} \quad \frac{V_T}{V_L} = \sqrt{\frac{1 - 2v}{2(1 - v)}} \tag{1}$$

Equation 1 shows that for a particular value of v the ratio V_T/V_L remains constant for all materials irrespective of their pore geometry or pore structure. It is well established now that besides porosity, different pore geometries also affect ultrasonic velocities differently [11]; therefore, it will be logical to assume that that pore geometry affects both longitudinal and shear velocities in an identical manner, and materials undergo similar morphology changes during sintering leaving porosity as the only relevant parameter affecting the velocity ratio.

For a material whose Poisson's ratio remains invariant with porosity, Eq. 1 shows that V_T is simply a linear function of V_L. For green or partially sintered compacts whose Poisson's ratio is lower than that of theoretically dense or pore-free material, Poisson's ratio must increase as sintering progresses with a decrease in velocity ratio and increase in V_L. On the other hand, for materials whose green compact's Poisson's ratio is higher than that of the pore-free material velocity ratio, V_L must increase with sintering with consequent decrease in Poisson's ratio. Figure 1 shows a plot of $\frac{V_T}{V_L}$ versus normalized longitudinal velocity V_L^* (normalized with respect to that of theoretically dense or pore-free material) for a number of ceramic and metallic materials [3, 21–24] prepared through powder processing route. In all cases the experimental data points fall on a straight line having coefficients of correlation varying from 0.912 to 0.998. Thus we assume a linear dependence of the velocity ratio on V_L^* given by the relation

$$\frac{V_T}{V_L} = \alpha + \beta V_L^* \tag{2}$$

where α, β are constants. For invariant Poisson's ratio $\beta = 0$ and the velocity ratio remains constant. This is the case for the data on RBSN reported by Thorp and Bushell [24]. The

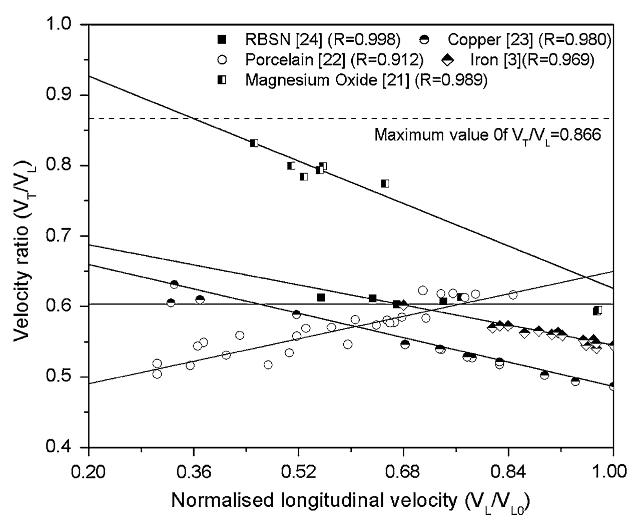

Fig. 1 Ultrasonic velocity ratio of different sintered materials plotted against normalized longitudinal velocity

value of Poisson's ratio is 0.201 irrespective of porosity and Eq. 2 gives a straight line parallel to V_L^*-axis as shown in Fig. 1. For $\frac{V_T}{V_L}$ decreasing with V_L, β becomes negative. Equation 2 shows that the variation of V_T with V_L during sintering can be predicted if the values of α and β are known and these values can be evaluated if ultrasonic velocity values at two points are known—that of fully sintered pore-free material and that of green compacts or partially sintered compacts. The velocity values for pore-free material may be estimated from mean polycrystalline (VRH) elastic moduli values where such data are available. The velocity values of green or partially sintered compacts are obtained from experimental measurements. However, to use the velocity measurements for monitoring density or porosity changes during sintering, its variation corresponding to velocity changes must be known. Variation of ultrasonic velocity with porosity is usually analyzed in terms of a power law equation [25] given by

$$V_X = V_{X0}(1 - ap)^{n_x} \tag{3}$$

where n_x and a are constants, p is the porosity, and X = L or T for longitudinal and shear velocity, respectively. The constant 'a' is related to the critical porosity (p_c) at which ultrasonic velocity vanishes, by the relation $a = \frac{1}{p_c}$. The value of p_c can only be in the range $0 < p_c \leq 1$; therefore, minimum value of a is 1.

The right-hand side of Eq. 3 contains two unknowns 'a' and n_x, and to determine the value of n_x uniquely at least $n_x + 1$ data point's values must be known. Moreover values of V_L and V_T calculated from Eq. 3 must satisfy Eq. 2. Therefore a relation correlating V_x, n_x and α, β is derived as follows:

$$\frac{dV_T}{dV_L} = \frac{dV_T}{dp}\frac{dp}{dV_L} \tag{4}$$

Evaluating the left-hand side from Eq. 2 and the right-hand side from Eq. 3 and substituting in Eq. 4 gives after mathematical simplification

$$\Gamma = n_T\left(\frac{V_T}{V_{T0}}\right)^{\left(\frac{n_T-1}{n_T}\right)} \tag{5}$$

where

$$\Gamma = n_L\left(\frac{V_{L0}}{V_{T0}}\right)\left(\alpha + 2\beta\frac{V_L}{V_{L0}}\right)\left(\frac{V_L}{V_{L0}}\right)^{\left(\frac{n_L-1}{n_L}\right)} \tag{6}$$

Equation 5 shows that a Ln–Ln plot of Γ versus $\frac{V_T}{V_{T0}}$ should give a straight line and the value of n_T can be obtained from the antilogarithm of the intercept on Ln(Γ) axis. However, to evaluate Γ, n_L and ($n_L + 1$) number values of V_L with corresponding values of V_T must be known. Thus the following procedure is adopted to find the values of n_L, n_T, and 'a' from Eqs. 5, 3, and 2.

An initial estimate of n_L is made from Eq. 3 using the measured values of longitudinal velocity and porosity of green/partially sintered materials taking the value of $a = 1$. A set of ten longitudinal velocity values including V_{L0} are generated by dividing the velocity values between V_{L0} and zero in ten equal intervals, and the corresponding values of V_T are then calculated from Eq. 2. Using these values of V_L and V_T and initial estimate of n_L, a Ln–Ln plot of Γ versus $\frac{V_T}{V_{T0}}$ is made and the linearity of the plot is checked through the value of coefficient of regression (COR). The value of 'a' is then incremented in steps of 0.001 giving a new estimate of n_L and Γ, and a new value of COR is calculated from the Ln–Ln plot. The value of 'a' is taken as the value for which COR becomes maximum. n_T is then calculated from the intercept. A minimum value of 0.950 for the COR is consider as the good fit. The estimation is made on the basis of ten data points on the assumption $n_T < n_L \leq 9$. It may be mentioned here this data fitting can be easily carried out on an Excel spread sheet in conjunction with a scatter diagram.

Change in density during sintering with corresponding change in V_L or V_T can be obtained from Eq. 3 by substituting the relation $p = 1 - \frac{\rho}{\rho_0}$ giving

$$\frac{\rho}{\rho_0} = \frac{(V_L^*)^{\frac{1}{n_L}} + a - 1}{a} = \frac{(V_T^*)^{\frac{1}{n_T}} + a - 1}{a} \tag{7}$$

Data analysis

Three data sets of ceramic materials and two of metallic materials, taken from the literature, have been analyzed using the procedure described above. These include two data sets of slip-cast alumina [4] and one each of uniaxially pressed porcelain [22], cold isostatically pressed copper [23], sintered and hot isostatically pressed iron [3]. Wherever green compact's data are not reported, the values corresponding to the reported highest porosity value have been considered as the value for the partially sintered compact.

Alumina

Two sets of data, analyzed here, are taken from Kulkarni et al. [4]. The green compacts were prepared by slip casting with different pH values of the slip. The data corresponding to pH values of 4.0 and 10.5 are analyzed here. Ultrasonic velocities and relative densities of green compacts are V_L = 1,881 m/s, V_T = 1,194 m/s, 62.9%, and V_L = 1,689 m/s, V_T = 1,071 m/s, 53.9% for pH 4.0 and 10.5, respectively (Table III of Reference [4]). Ultrasonic velocities of theoretically dense alumina are estimated to be V_L = 10839.0 m/s and V_T = 6392.8 m/s

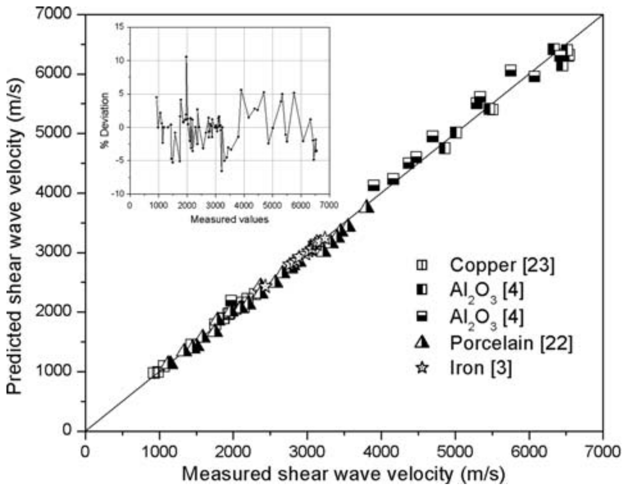

Fig. 2 Predicted shear velocities compared with the measured ones. The inset shows the percentage deviation from the measured values

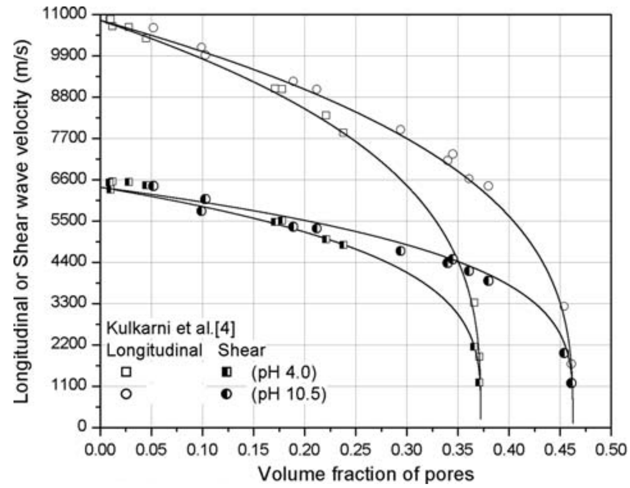

Fig. 3 Longitudinal and shear velocities of alumina versus porosity. Solid line corresponds to predicted values

from mean polycrystalline (VRH) values of bulk modulus $K_0 = 251.0$ GPa and $G_0 = 162.9$ GPa as reported by Anderson et al. [26]. Using these values of ultrasonic velocities, (α, β) values are evaluated from Eq. 2 as (0.644, −0.054) and (0.716, −0.126) for data sets having pH 4.0 and pH 10.5, respectively. Predicted values of V_T calculated from Eq. 2 based on these values of (α, β), corresponding to the measured values of V_L at different porosities (Table IV of Reference [4]) are compared in Fig. 2 along with its percentage of deviation (shown in the inset) from the measured ones. The agreement between the two is extremely good. In all cases percentage deviations lie within ± 5% of the measured values except for one data point where it deviates by +10%.

The values of parameters (a, n_L, n_T) in Eq. 3 are evaluated from Eq. 5 following the method described earlier. These are (2.685, 0.318, 0.268) and (2.162, 0.328, 0.262) corresponding to pH 4.0 and pH 10.5 data sets, respectively. In all cases COR of $\mathrm{Ln}(\Gamma)$ versus $\mathrm{Ln}\left(\frac{V_T}{V_{T0}}\right)$ are obtained as 1. Figure 3 compares the predicted variation of ultrasonic velocity with porosity based on Eq. 3 with the experimentally measured ones showing excellent agreement between the two.

Copper

The data analyzed here are those reported by Yeheskel et al. [23]. The green compacts were prepared from 2 μm to 3 μm sized copper powder by cold isostatic pressing, and then they were sintered in the temperature range 270–473 °C. For further details one can refer to their papers [23, 27]. The ultrasonic velocity values of the compact pressed at 100 MPa and having porosity of ≈37% are treated as the green compact data. The theoretical density and the ultrasound velocities of pore-free polycrystalline copper [28] are taken as $\rho_0 = 8{,}960\ \mathrm{kgm^{-3}}$, $V_{L0} = 4{,}726\ \mathrm{ms^{-1}}$, and $V_{T0} = 2{,}298\ \mathrm{ms^{-1}}$. From these data on green compact and pore-free material, Eq. 2 gives the values of α, β as 0.703, −0.216, respectively. Predicted values of V_T from Eq. 2 are again compared with the measured values in Fig. 2 along with its percentage deviation from the measured ones. There is an excellent agreement between the two with the maximum deviation of 4.5% from the measured one. The values of parameters are evaluated as before, giving values of $a = 2.618$, $n_L = 0.240$, $n_T = 0.293$, and COR of $\mathrm{Ln}(\Gamma)$ versus $\mathrm{Ln}\left(\frac{V_T}{V_{T0}}\right)$ as 0.996. Equation 3 corresponding to these values along with the experimental data are compared in Fig. 4. For both longitudinal and shear wave velocities predicted values show satisfactory agreement with the data. However, in both the

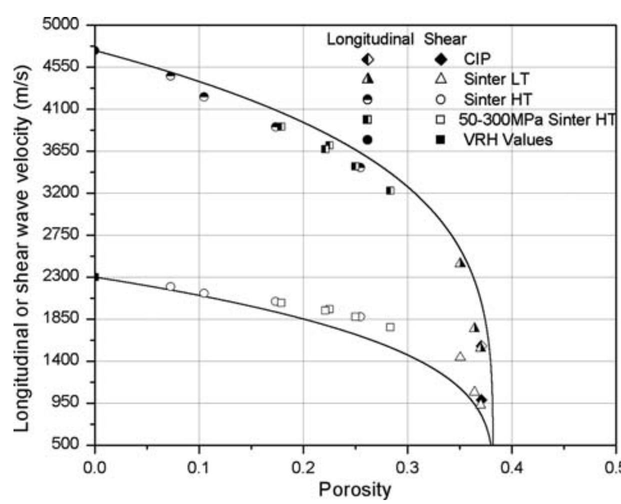

Fig. 4 Longitudinal and shear velocities of copper versus porosity. Solid line corresponds to predicted values

cases the theory correctly predicts the trend of variation of velocities with porosity.

Iron

Iron compacts data [3] that are analyzed here, were sintered and hot isostatic pressed in the pressure range of 1,200–200 MPa and the temperature range of 1,523–1,250 °C. Since green compact data have not been reported the data point corresponding to compaction pressure of 200 MPa and the sintering temperature of 1,250 °C with a pore volume of 21.6% are considered as the partially sintered data. The velocities are calculated from the reported values of Young's and shear moduli using the well-known relations [3] of the physical acoustics theory. The density and velocity values of pore-free material [29] are taken as ρ_0 = 7,860 kgm^{-3}, V_L = 5,960 ms^{-1}, and V_T = 3,240 ms^{-1}. From Eq. 2 the values of α,β work out to be 0.723, −0.178, respectively. Predicted values of shear velocities are compared with the measured ones in Fig. 2 and show excellent agreement between the two (Fig. 5). In no case does predicted value differ from the measured ones by more than 1.6%. The values of parameters are evaluated as before, giving values of $a = 3.125$, $n_L = 0.344$, n_T = 0.296, and COR of Ln(Γ) versus $\mathrm{Ln}\left(\frac{V_T}{V_{T0}}\right)$ as 0.999. Figure 6 compares the predicted variation of ultrasonic velocities with porosity, with the experimental data showing excellent agreement between the two.

Porcelain

Boisson et al. [22] have reported ultrasonic properties of uniaxially pressed porcelain. However, for this data set

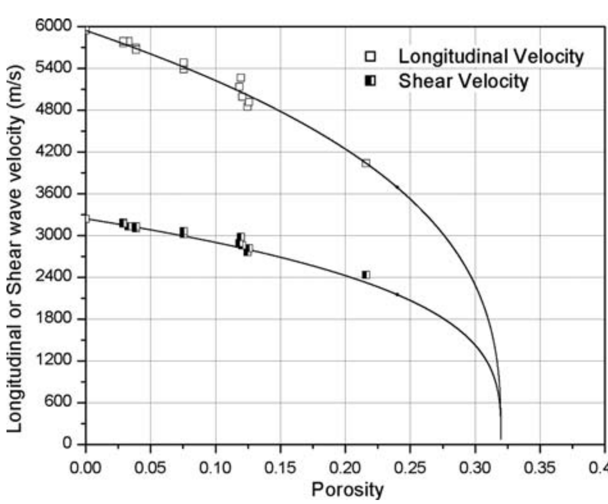

Fig. 5 Longitudinal and shear velocities of iron versus porosity. Solid line corresponds to predicted values

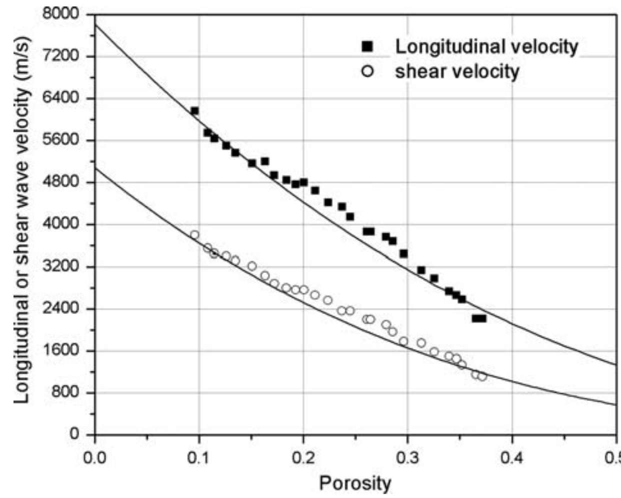

Fig. 6 Longitudinal and shear velocities of porcelain versus porosity. Solid line corresponds to predicted values

neither the green compact data nor the pore-free material properties are available. Therefore, the reported data corresponding to the highest porosity of ≈37% are considered as the partially sintered compact. The pore-free material values are estimated from the linear explorations of low porosity data as V_L = 7,820 ms^{-1} and V_T = 5,080 ms^{-1}. Based on these values Eq. 2 gives values of α, β as 0.450, 0.199, respectively. In this case β is positive, indicating that $\frac{V_T}{V_L}$ increases with sintering, i.e. with increase in V_L. Predicted shear wave velocities are again compared with the measured ones in Fig. 2. They are in excellent agreement with the measured ones with a maximum deviation of ≈5%. The values of a, n_L, n_T evaluated from Eq. 5 work out to be 1, 2.551, 3.139, respectively, with a COR of 0.999 between Ln(Γ) versus $\mathrm{Ln}\left(\frac{V_T}{V_{T0}}\right)$. The predicted variation of velocities with porosity is compared with the experimental data in Fig. 6 showing reasonably good agreement between the two.

Discussion

Based on the analytical procedure described here ultrasonic velocity variation with porosity (relative density = $1-p$) during sintering can be predicted from the properties of green compacts reasonably accurately. However, a more rigorous test of this procedure is the prediction of Poisson's ratio variation with porosity. This is shown in Fig. 7 along with the experimental values. Predicted variation is calculated from Eqs. 1, 2, and 3. Poisson's ratio for the only set of alumina data (Kulkarni et al. [4] (pH 4.0)) has been shown to maintain the clarity of the plot. The other set provides equally good agreement with the predicted values.

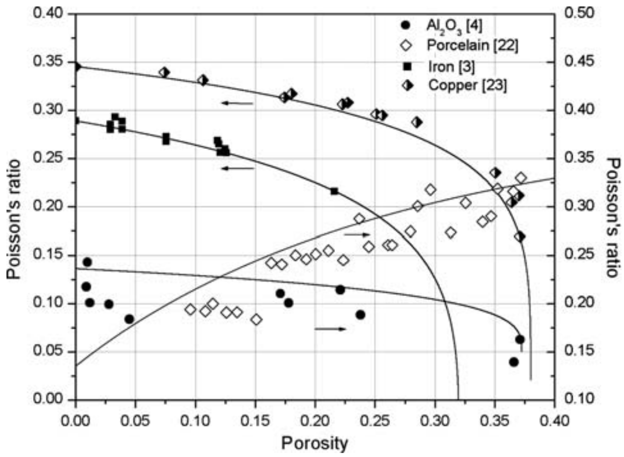

Fig. 7 Poisson's ratio of alumina, copper, iron, and porcelain versus porosity. Solid line corresponds to predicted values

It may be noted that the increasing trend of Poisson's ratio with porosity for porcelain is also correctly predicted. The agreement between the experimental and the predicted values can be considered extremely good, considering the error involved in the estimation of Poisson's ratio as it calculated as the difference of almost two equal quantities.

From what has been presented above it seems ultrasonic properties of the sintered compact are predetermined based on the values of green or partially sintered compact. But why should it be uniquely predetermined at the green compaction stage itself ? A possible explanation may be as follows:

The ultrasonic as well as elastic properties of the green powder compact in its initial stage of formation, when the particles are just in contact with each other, will depend on the powder morphology and the particle-to-particle contact geometry. This in turn will determine the microstructure of the compact. Rothenburg et al. [30] have shown that for granular materials having frictional interfaces, an applied force can have a tangential component along the plane of contact and Poisson's ratio of such a system is given by

$$v = \frac{1 - \lambda}{4 + \lambda} \tag{14}$$

where λ is the ratio of tangential-to-normal contact stiffness. Since the ultrasonic velocity ratio is related to v by Eq. 1, it is logical to assume the ultrasonic velocity ratio is also dependent on λ. For green compacts having $\lambda < 1$, Poisson's ratio will increase with decrease in velocity ratio if λ decreases further during sintering and vice versa. In this case the velocity ratio is given by a linear function of λ to a first-order approximation. Green compacts having values of λ greater than one (i.e. the tangential contact stiffness is greater than normal contact stiffness) will have a negative Poisson's ratio. As pointed out by Rothenburg et al. [30] "any assembly of particles with nonconvex surfaces that allow sufficient interpenetration should show a negative Poisson's ratio." This is also supported by the experimental evidences [21, 31] in the literature where negative Poisson's ratio values have been reported for high values of porosity. In this case Poisson's ratio will decrease with increase in velocity ratio if sintering increases the value of λ and vice versa. Therefore, as the neck growth takes place with the progress in sintering, the stiffness ratio λ changes with consequent change in the velocity ratio depending on the value of λ of the green compact. Martin and Rosen [32] have studied the correlation between surface area reduction and ultrasonic velocity in sintered zinc powder compacts. Their results indicate that, over the entire range of porosities, from completely unsintered to the onset of pore closure, the surface area reduction is linearly related to longitudinal ultrasonic wave velocity. They [32] have also observed that the initial stage of sintering is characterized by interparticle neck growth and therefore surface area reduction without densification. In the intermediate stage of sintering, bulk transport mechanisms become more active and neck growth is accompanied by a reduction in porosity. Over both these stages of sintering the linear relation between surface area reduction and longitudinal wave velocity remains valid indicating strongly that the reduction in specific surface area and the increase in longitudinal wave velocity depend in a similar way on the changes in interparticle neck geometry [32]. This is further supported by the TEM study made by Yeheskel et al. [29] of the sintered copper powder. The elastic moduli of copper compacts start increasing above about 350 °C sintering temperature with only limited increase in relative density suggesting that the elastic moduli depend on factors other than the density, such as the microstructure of the interparticle contact area [29]. Since interparticle neck geometry also controls the velocity ratio as explained above, the assumption of linear variation of velocity ratio with longitudinal wave velocity in Eq. 2 provides reasonable agreement with the experimental data. The sintering characteristics of the material bring in geometric changes at contact points of powder which determine the change in initial pore morphology. Therefore the change in the geometry of the solid framework through neck growth should be considered as the cause and its effect is the change in pore morphology and not vice versa. Of course, this excludes material with pore formers. It is the solid frame work which determines the ultrasonic properties Thus contact stiffness ratio λ and contact point geometry of the compact play a dominant role in determining ultrasonic properties of the sintered products.

It may be mentioned here that the present procedure can be extended for estimation of elastic properties using the well-known relations given by the theory of physical acoustics.

Conclusion

A new method for estimation of ultrasonic properties of porous ceramics based on the properties of green/partially sintered compacts has been presented. However, the ultrasonic properties of the theoretically dense or pore-free material must be known. The study shows that the ratio of ultrasonic shear wave velocity to longitudinal velocity is a function of porosity only and is given by a linear function of longitudinal velocity. The method may be used as a potential tool for quality control of sintered materials.

Acknowledgements The author wishes to thank Director, CGCRI, for his permission to publish this paper.

References

1. Nagarajan A (1971) J Appl Phys 42:3693
2. Green DJ, Nader C, Brenzy R (1990) Ceram Trans 7:345
3. Panakkal JP, Willems H, Arnold W (1990) J Mater Sci 25:1397
4. Kulkarni N, Moudgil B, Bhardwaj M (1994) Am Ceram Soc Bull 73:146
5. Generazio ER, Roth DJ (1989) J Am Ceram Soc 72:1282
6. Papadakis EP, Patersen BW (1979) Mat Eval 37:76
7. Arons RM, Kupperman DS (1982) Mat Eval 40:1076
8. Panakkal JP, Ghosh JK, Roy PR (1984) J Phys D: Appl Phys 17:1791
9. Maitra AK, Phani KK (1994) J Mat Sci 29:4415
10. Baaklini GY, Generazio ER, Kiser JD (1989) J Am Ceram Soc 72:383
11. Rice RW (1998) Porosity of Ceramics, Marcel Dekker Inc, New York
12. Waterman PC, Truell R (1961) J Math Phys 2:512
13. Ying CF, Truell R (1956) J Appl Phys 27:1086
14. Sayers CM, Smith RL (1982) Ultrasonics September:201
15. Hill R (1965) J Mech Phys Solid 13:213
16. Budiansky B (1965) J Mech Phys Solid 13:223
17. Wu TT (1966) Int J Solid Struct 2:1
18. Berryman LG (1980) J Acoust Soc Amm 68:1820
19. McLaughlin R (1977) Int J Engg Sci 15:237
20. Martin LP, Dadon D, Rosen M (1996) J Am Ceram Soc 79:1281
21. Hanna RK, Crandell WB (1962) Am Ceram Soc Bull 41:311
22. Boisson J, Platon F, Boch P (1976) Ceramurgia anno VI:74
23. Yeheskel O, Pinkas M, Dariel MP (2003) Mater Lett 57:4418
24. Thorp JS, Bushell TG (1985) J Mater Sci 20:2265
25. Mukhopadhyay AK, Phani KK (2000) J Eur Ceram Soc 20:29
26. Anderson OL, Schreiber E, Lirberman RC, Soga N (1968) Rev Geophys 6:491
27. Yeheskel O (2006) Quantitative NDE of the Young's modulus of FCC porous metals—presented at 12th A-PCNDT 2006—Asia-Pacific Conference on NDT, Auckland, New Zealand
28. Anderson OL (1965) In: Mason WP (ed) Physical Acoustics, vol III, partB. Academic Press, New York
29. Mason WP (1958) Physical acoustics and the properties of solids. Von Nostrand Co. Inc., Princeton
30. Rothenburg L, Berlin AlAl, Bathurst RJ (1991) Nature 354:470
31. Spinner S, Knudsen FP, Stone L (1963) J Res Natl Bur Std Sect C 67:39
32. Martin LP, Rosen M (1997) J Am Ceram Soc 80:839